Shock compression and isentropic release of rhyolite

W. Yang, G. Chen, W. W. Anderson, and Thomas J. Ahrens

Citation: AIP Conference Proceedings **309**, 1115 (1994); doi: 10.1063/1.46484
View online: http://dx.doi.org/10.1063/1.46484
View Table of Contents: http://scitation.aip.org/content/aip/proceeding/aipcp/309?ver=pdfcov
Published by the AIP Publishing

SHOCK COMPRESSION AND ISENTROPIC RELEASE OF RHYOLITE

W. Yang, G. Chen, W. W. Anderson and Thomas. J. Ahrens
Lindhurst Laboratory of Experimental Geophysics, Seismological Laboratory
California Institute of Technology, Pasadena, CA 91125

A series of shock compression experiments have been conducted on rhyolite at pressure ranging from 6 to 33 GPa. A velocity interferometer (VISAR) was employed to monitor the particle velocity of an aluminum reflector with a diffused surface bonded to the rhyolite sample. In the forward ballistic experiments, a slow rise shock wave front is observed at 6 GPa. While in the forward experiments their release waves are smeared, in a reverse ballistic experiment, the particle velocity variation at the shock wave plateau and the isentropic release wave arrival have been clearly observed. Using Swegle's mixed phase model, we simulated the experimental results with WONDY code. Like quartz and granite, the rhyolite data could be fit to a frozen release model which has some hysteric behavior. The Eulerian sound velocity at shock pressure 8.7 GPa has been determined to be 5.6 km/s.

INTRODUCTION

The shock loading and unloading of silicate geological materials are of interest for the description of impact and explosively driven shock waves in crustal rock. Shock propagation in quartz have been studied extensively at pressures up to 650 GPa by Trunin et al [1], Al'tshuler et al [2], Wackerle [3] and Fowles [4]. Release isentropes have been measured by Grady et al [5] in quartz-bearing rock, Grady and Murri [6] in feldspar, and by Poderets et al [7] and Chhabildas [8,9] in single crystal quartz. It has been found that the phase transition from quartz to stishovite occurs in mixed phase region from 14 to 40 GPa. Upon isentropic release, the high density phase does not immediately undergo the reverse transformation to the low density quartz phase. Recently, Swegle [10] constructed a thermodynamically consistent mixed phase model which can be used to analyze loading and unloading shock wave data in quartz-bearing rocks and reported several data for granite and rhyolite. The release behavior of rhyolite was previously less well studied. We conducted a series of release isentrope measurements on rhyolite, using a VISAR [11] to monitor the compression and release particle velocities of an Al buffer bonded to a rhyolite sample. Numerical simulations with WONDY code [12] were conducted and used to fit the data. The Eulerian sound velocity of rhyolite at high pressure in one reverse ballistic experiment was also determined.

EXPERIMENTS

The VISAR used in the present experiments incorporated the push-pull modification [13] for improved signal quality. The time resolution of the data are ~3 ns and the velocity precision ~1%. Two type of experiments have been conducted----forward and reverse ballistic. The forward ballistic target assembly (Figure 1a) consists of an aluminum driver plate (2 mm thick), a rhyolite target (6 mm thick), a diffuse reflecting Al2024 or Al6061 buffer (0.8 mm thick) and a LiF window (12 mm thick). The flyer plate used are Al2024 (5 mm thick) and W (4 mm thick). For the reverse ballistic experiment, the flyer plate was rhyolite and it impacted the Al6061 buffer directly (Figure 1b). Table 1 lists the experimental parameters.

RESULTS AND SIMULATIONS

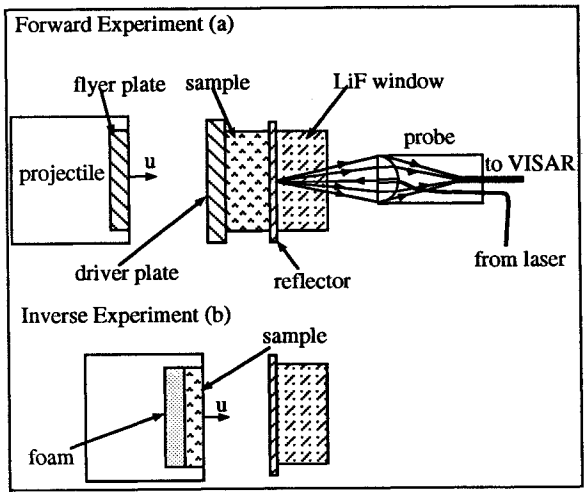

Figure 1. Experimental assembly.

Table 1. Experimental Parameters

I. Forward Ballistic Experiments		
Shot No.	Flyer plate velocity (km/s)	Rhyolite sample density (g/cm^3)
886	1.45 (Al2024)	2.298
887	1.06 (Al2024)	2.29
888	1.97 (Al2024)	2.29
896	2.55 (W)	2.35
II. Reverse Ballistic Experiment		
Shot No.	Rhyolite flyer velocity (km/s)	Rhyolite sample density (g/cm^3)
895	1.48	2.28

The forward ballistic experimental results are shown in Figure 2. At low pressure 6 GPa, the shock wave front rises very slowly (~280 ns), make it very difficult to determine the elastic precursor's amplitude. The observed low amplitude precursor is due to the strength of the Al buffer. As pressure increases, the shock front rise-time becomes shorter. For shock pressures >9 GPa, the wave front becomes nearly a step function. The long rise time at low pressures arises from heterogeneity of the rhyolite sample. The grain size is up to a few millimeters. The particle velocities at the shock wave plateau and

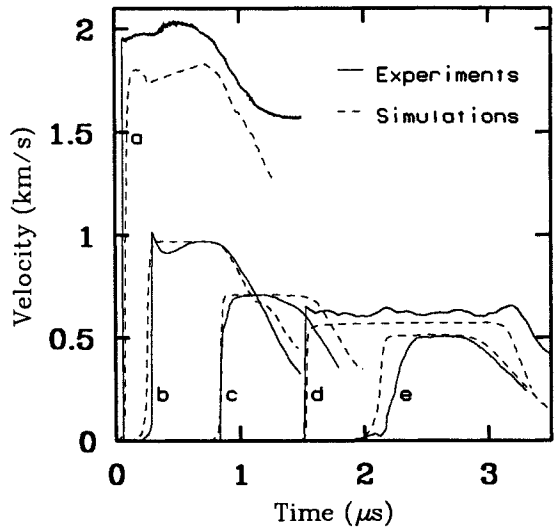

Figure 2. Particle velocity profiles. a. shot 896, 33 GPa; b. shot 888, 12 GPa; c. shot 886, 8.7 GPa; d. shot 895, 8.7 GPa; e. shot 887, 6 GPa.

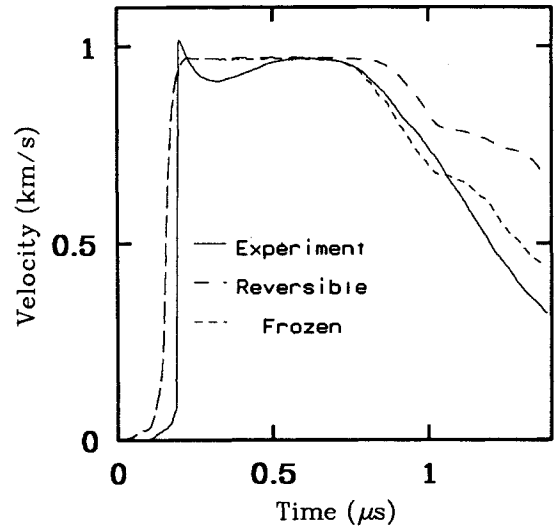

Figure 3. Comparison of simulation models. The frozen model clearly fits better than the reversible one.

release region, however, are smoothed out by the complex wave reflections between different layers of materials. The gradual velocity increase of Figure 2a is due to the compression wave reflected from the W flyer plate. The dashed lines are numerical simulation results using the

Table 2. Rhyolite Equation of State Parameters

	LPP	HPP
ρ_0(g/cm^3)	2.50	4.21
K_0(GPa)	37.0	350
K_0'	6.27	3.3
γ_0	0.7	1.2
ν	0.2	
Y_0(GPa)	2.1	

LPP-low pressure phase; HPP-high pressure phase; γ_0-Gruneisen's parameter; ν-Poisson's ratio.

WONDY code and Swegle's mixed-phase model. The strength of rhyolite is obtained from a streak camera experiment which provided the Hugoniot elastic limit of 2.8 GPa. Rhyolite is assumed frozen during release region (that is, when pressure decreases, high density phase will not transform back to low density phase). The mixed phase region is chosen as 5-41 GPa. A reversible model is also used, but the frozen model best fits the experimental particle velocity profile (Figure 3). In our simulation model, the sample porosity is closed when pressure reaches 1 GPa. Rhyolite parameters used in the simulation are given in Table 2. Dynamic strength Y_0, bulk modulus K_0 and its derivative K_0' are obtained from our impedance match [14] experiments. The experimental particle profile and simulation for the reverse ballistic experiment is shown in Figure 2d. The oscillation of the particle velocity at the shock wave plateau reflects the heterogeneity of the sample. The clear onset of the release wave makes it possible to calculate the sound velocity of rhyolite at high pressure. The high pressure sound velocity of Al6061 is provided by Duffy [15]. The Eulerian sound velocity for this shot was determined to be 5.6 km/s at 8.7 GPa. Due to the heterogeneity of the sample, it is unclear whether this is a longitudinal or bulk release wave. Figure 4 shows the simulation of the isentropic release trajectories of rhyolite from Hugoniot states similar to our

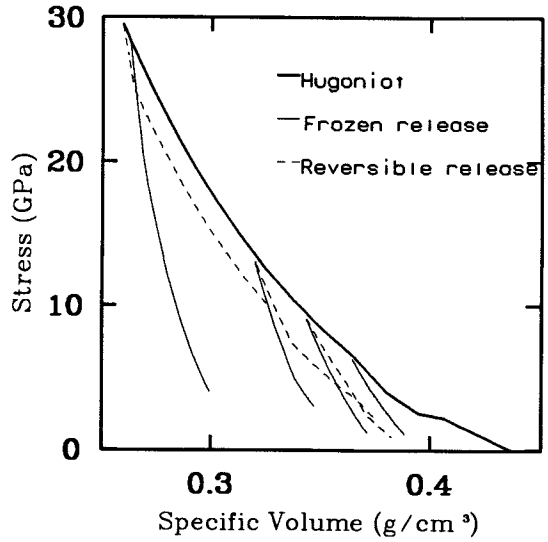

Figure 4. Isentropic release curves of rhyolite.

experiments on the pressure volume plane. The hysteric frozen release behavior can cause strong attenuation of shock wave propagation.

CONCLUSIONS

Like quartz and granite, rhyolite appears to have release isentrope trajectory which is frozen up to 33 GPa. Sample heterogeneity causes slow wave front rise at low shock pressures. Particle velocity oscillation has been observed at the shock wave plateau. Eulerian sound velocity of rhyolite at shock pressure 8.7 GPa is determined with a reverse ballistic experiment.

ACKNOWLEDGMENTS

This research is supported under Contract F49670-92-J-0402 and Mission Research Corp. Subcontract #SC-0064-90-0002. Division of Geological and Planetary Sciences Contribution #5325.

REFERENCES

[1] R. F. Trunin and G. V. Simakov et al,

Dynamic compressibility of quartz and quartzite at high pressure, *Izv. Acad. Sci. USSR Phys. Solid Earth*, no. 1, p. 13-20,1971.

[2] L. V., Al'tshuler et al, Shock-wave Compression of periclase and quartz and the composition of the earth's lower mantle, *Izv. Acad. Sci. USSR Phys. Solid Earth*, no 10, pp. 657-660,1965.

[3] J. Wackerle, Shock-wave compression of quartz, *J. Apply. Phys.*, 33, p. 922-937, 1962.

[4] G. R. Fowles, Dynamic compression of quartz, *J. Geophys. Res.*, 72, p. 5729-5742, 1967.

[5] D. E. Grady, Shock deformation of brittle solids, *J. Geophys. Res.*, 85, B2, p. 913-924, 1980.

[6] D. E. Grady et al, Quartz to stishovite: Wave propagation in the mixed phase region, *J. Geophys. Res.*, 79, p. 332-338, 1974.

[7] M. A Podurets et al., *Izv. Acad. Sci. USSR Phys. Solid Earth*, no. 12, p. 419-424, 1976.

[8] L. C. Chhabildas and D. E. Grady, Dynamic material response of quartz at high strain rates, in *Mat. Res. Soc. Symp. Proc. Vol. 22*, edited by C. Homan et al, North Holland, Elsever Science Publishing, 1984, p.147.

[9] L. C. Chhabildas, Shock loading and release behavior of X-cut quartz, in *Shock Waves in Condensed Matter*, edited by Y. M. Gupta, Plenum Publishing Corp., 1986.

[10] J. W. Swegle, Irreversible phase transitions and wave propagation in silicate geologic materials, SAND89-1443,1989.

[11] L. M. Barker and R. E. Hollenbach, Laser interferometer for measuring high velocities of any reflecting surface, *J. Appl. Phys.*, 43, p. 4669-4675, 1972.

[12] M. E. Kipp and R. J. Lawrence, WONDY V - A one-dimensional finite-difference wave propagation code, SAND81-0930, 1982.

[13] W. F. Hemsing, Velocity sensing interferometer (VISAR) modification, *Rev. Sci. Instrum.*, 50, p. 73-78, 1979.

[14] T. J. Ahrens, in *Methods of Experimental Physics*, New York: Academic Press, 1987, Vol. 24, Part A, p. 185-234.

[15] T. S. Duffy, Elastic properties of metals and minerals under shock compression, Ph. D thesis, California Institute of Technology, 1992, pp. 296.